Indian Journal of Chemistry
Vol. 60A, July 2021, pp. 915-926

Synthesis, spectral characterisation and pharmacological studies on Co(II), Ni(II), Cu(II) and Zn(II) bis-Schiff base complexes derived from 4-hydroxybenzohydrazide

P Priya[a], P Jayaseelan[b] & S Vedanayaki[a,]*

[a]Department of Chemistry, Kandaswami Kandar's College, Paramathi-Velur, Tamil Nadu 638 182, India

[b]Chemical Division, Mettur Thermal Power Station-2, Mettur Dam, Tamil Nadu 636 406, India

*E-mail: varshuvishal@gmail.com

Received 08 February 2021; revised and accepted 12 April 2021

The transition metal(II) chelates have been prepared by the reactions of bis-Schiff base ligands derived from 4-hydroxy benzohydrazide and isophthalaldehyde/ o-phthaldehyde in 1:1 metal to ligand ratio. The formed ligands and their metal complexes have been investigated by elemental analysis, different spectroscopic and thermal analyses techniques. The low molar conductance values give the non-electrolytic nature of the metal(II) chelates. From the spectroscopic observations of complexes, the molecular formula is found to be $[M(L_n)_2Cl_2]$ (where M= Co(II), Ni(II), Cu(II) and Zn(II), n=1 and 2) and the tetradentate N_2O_2 donor sites of ligands is attached to the metal centre. The docking results predicts that the protein with ligands have good interaction energy. All formed complexes have efficient antibacterial activity than ligand for tested pathogens. The mode of binding interaction of ct-DNA and Cu(II) complexes gives the intercalative binding with hypochromism shifts using electronic titrations method. In electrophoresis, cleavages of PUC18DNA to cleave effectively with Cu(II) complexes in the presence of hydroxyl radicals. The antioxidant assay of DPPH radical scavenging activity of tested compounds shows good results, when compared to ascorbic acid as standard. The anticancer MTT assay of Cu(II) complexes tested against MCF-7 cancerous cells gives the promising therapeutic activity.

Keywords: Bis-Schiff base, Docking, DNA binding and cleavage, Antioxidant, Anticancer activity

Forthcoming days, cancer is a crucial problem in human health and causes a huge financial expense throughout the world. The world health organisation calculates that twelve million deaths worldwide will be due to cancer by 2030[1]. Metal based like cisplatin anticancer drug plays a leading role in the treatment of various malignant tumors, but serve as various side effects. Therefore, our aim is to prepare the chemotherapeutic drugs without side effects or fewer side effects[2]. This problem of cisplatin originates due to binding mode of covalent cross-links with DNA[3]. These disadvantages have motivated the chemists to develop novel metal compounds with improved pharmacological properties based on different metals and ligands[4,5].

Drug isomerism in research field has opened a new era of drug development. Currently, the knowledge of isomeric complexes has helped us to introducing the more efficient drug alternatives of the newer as well as existing drug[6]. Generally, the small molecules can react with DNA via covalent or non-covalent interactions. There are several types of sites in the DNA molecules where such binding can occur like (i) between two base pairs (intercalation), (ii) in the minor groove, (iii) in the major groove or (iv) on the outside of helix[6].

Metal complexes derived from hydrazine Schiff base are exhibiting an efficient of DNA syntheses by binding via intercalation mode[7]. The formation of intercalation mode which is favoured by the planarity of complexes due to interaction between planar aromatic ring and base pairs of DNA[8,9], besides than other factors like size, nature of ligand, hydrophobicity, electron density of interacting aromatic rings and the geometry of complex, all played important roles[10]. Literatures reveal that Schiff base complexes of hydrazone exhibited such type of interactions; play an essential role as enzyme inhibitor, anticancer and antioxidants[11]. This intercalation is the main purpose of studying towards the design and development of new effective drugs. In recent days, the chemistry of hydrazone derivative ligand has gained much attention because of their structures with more than two donors presented in

their relative positions which may serve as multi-coordination sites and form stable chelates with essential metal ions[12,13]. Moreover, hydrazone exhibit a vital role in enhancing the selectivity and lethality profile of certain drug candidates. A vast content of literature is present on hydrazone type ligands unfolding their fascinating properties[14] and also, a variety of polydentate chelates of these ligands have been reported to possess different co-ordination behaviour with different metal atoms[15]. The hydrazones are important class of Schiff base ligands, which have attracted attention of medicinal chemists due to their wide ranging biological and pharmaceutical properties such as anticancer, antimicrobial, antiviral and herbicidal properties[4,16]. Recent researches, there is an increasing interest in design and preparation of bis-hydrazones alongside with their metal complexes because of their chemical applications in biological fields[17].

Based on this background, in the study the novel monometallic complexes derived from 4-hydroxy-benzohydrazide with isomers of isophthalaldehyde/ o-phthaldehyde were synthesised and characterised by elemental, molar conductance, UV, FT-IR, ^{1}H NMR, ESR, ESI-MS, magnetic measurement and thermal studies. The synthesised bis-Schiff base hydrazone ligands and its metal complexes were successfully tested for docking, in vitro antibacterial, antioxidant, DNA cleavage properties. DNA binding and in vitro anticancer activity of human breast cancer MCF-7 cell line was also tested for the synthesised Schiff base Cu(II) complexes.

Materials and Methods

The analytical grade chemicals and reagents are used for this work are 4-hydroxybenzohydrazide (≥97% Merck), isopthaladehyde (98%, LOBA Chemie), o-phthalaldehyde (97.5%, Merck), hydrated metal chlorides ($CoCl_2.6H_2O$, $NiCl_2.6H_2O$, $CuCl_2.2H_2O$, $ZnCl_2.H_2O$), methanol (98%, Merck) and hydrochloric acid (AR grade). All chemicals were used for without further purification.

Synthesis of bis-Schiff base ligands (1 & 2)

The Schiff base ligands were prepared by the mixture of isophthaladehyde **1**/ o-phthaldehyde **2** (0.01 mol) and 4-hydroxybenzohydrazide (0.02 mol) in 1:2 molar ratio was stirred in 20 mL methanol followed by 5-6 drops of conc. HCl added[18] and the mixture was refluxed at 60 °C for 4 h. The resulting coloured solution was kept in room temperature; the obtained precipitate was filtered, washed with methanol and dried under vacuum.

Synthesis of metal complexes

To a 20 mL of methanolic solution ligand (0.01 mol) with metal chlorides (0.01 mol) like cobalt(II) chloride hexahydrate ($CoCl_2.6H_2O$)/ nickel(II) chloride hexahydrate ($NiCl_2.6H_2O$)/ copper(II) chloride dihydrate ($CuCl_2.2H_2O$)/ anhydrous zinc(II) chloride ($ZnCl_2$) were separately stirred in 1:1 molar ratio and the reaction mixtures was refluxed for 4 h at 70 °C[19]. The obtained coloured precipitate was filtered, washed with methanol followed by diethyl ether, dried under vacuum (Scheme 1).

Instrumentation

The following instrument techniques were used to characterise the synthesised Schiff base ligand and their complexes. The functional groups are presenting in the compounds were investigated on SHIMADZU model FT-IR spectrometer and the percentages of elements like C, H and N were determined on Flash 1112 series elemental analyzer. The molecular masses of ligand complexes were measured by positive mode of Q-TOF ESI-Mass spectrometer. The magnetic moment values of unpaired electrons were calculated by Gouy's balance using a callibrant $Hg[Co(SCN)_4]$. In ligands, the chemical environment of protons was recorded on Bruker Advance ^{1}H NMR (300 MHz) spectrometer. The absorbance of compounds was noted on Perkin Elmer Lambda spectrometer in the range of 800-200 nm. For finding the number of unpaired electron of complex the study was performed by using JES-FA200 ESR spectrometer at room temperature used as standard tetracyanoethylene. Thermal studies were performed with DSC-TGA Universal 4.5A instrument the range of 30-800 °C at heating rate 20 °C in atmospheric air. AutoDock 4.2.2 package was used for docking calculations and the protein structure of *Staphylococcus aureus* (PDB 1D: 2DHN) was downloaded from protein data bank.

Testing procedure for antibacterial activity

The antibacterial activities were employed by disc diffusion method and the all synthesised compounds were tested against pathogens of gram positive bacteria: *Staphylococcus aureus* and *Bacillus subtilis* strains, gram negative bacteria: *Klebsiella pneumoniea* and *Escherichia coli* strains. The nutrient agar medium was dispersed homogenously after mixed

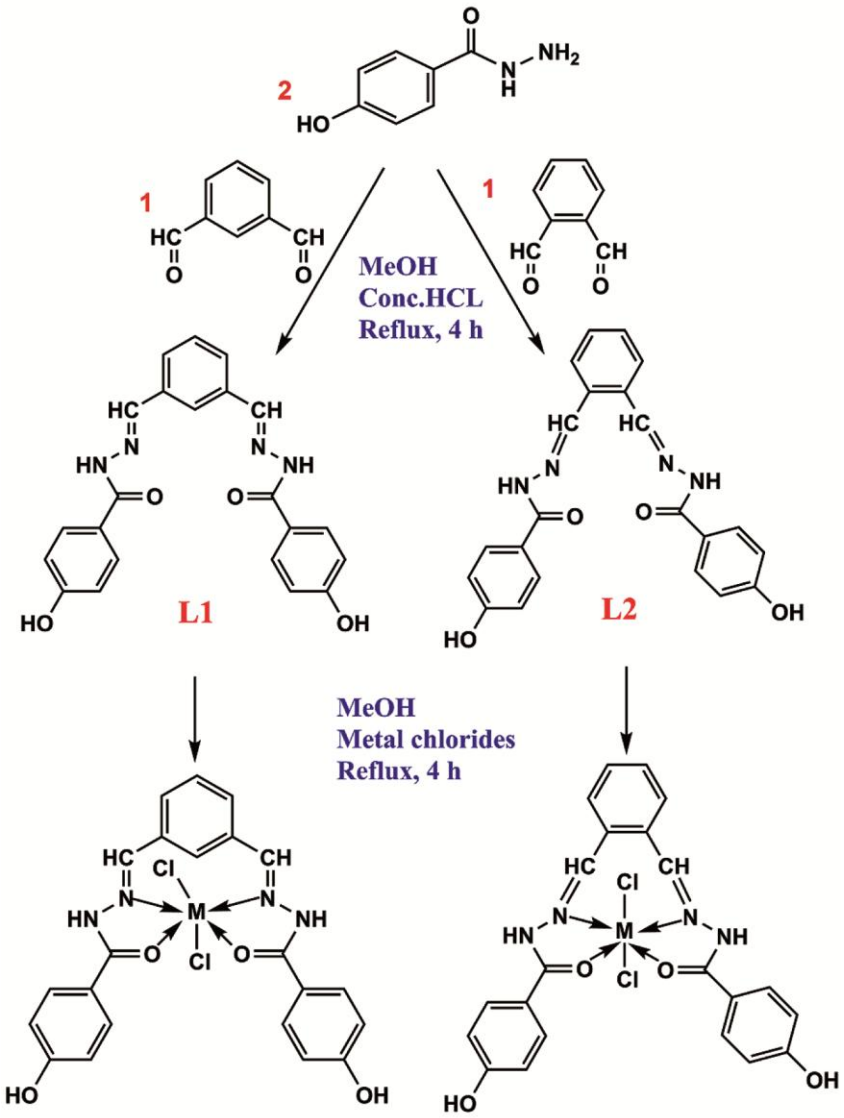

Scheme 1 — Structure of synthesised ligand 1, 2 and their metal complexes

with distilled water. The whole medium was shifted to the Petri-plates, where the filter paper was placed on disc. 100 µL of sample was poured on separately and incubated at 37 °C for 24 h. A clear inhibition of zone was occurred in the circle form and was measured by diameter in nm. Zone of inhibition was compared with standard drug using Tetracycline in DMSO solvent[20].

DNA interaction study

The absorption titration experiments of DNA interaction of Cu(II) complex was performed in UV-visible absorption spectrometer using calf thymus (ct) DNA. The stock solution of ct-DNA was prepared by dissolving it in Tris-HCl/NaCl solution (5 Mm Tris HCl/50 Mm NaCl, pH 7.5) at different concentration. The ct-DNA concentration was determined by measuring the absorption intensity 265 nm with molar absorption co-efficient (ε) of 6600 M^{-1} cm^{-1}. The stock solution of Cu(II) complex was made with 10% methanol and 90% buffer (Tris-HCl/NaCl, ct-DNA) solution in constant concentration (100, 120,140, 160, 180 µM). The absorption of Cu(II) complex was carried out by the absence and presence of ct-DNA. The absorption titration was measured by successive increasing DNA concentration. In order to eliminate the absorption of DNA itself, an equal amount of DNA was subsequently used as references[21].

DNA cleavage study

The studies of supercoiled plasmid PUC18DNA cleavage was performed by the synthesised ligands and their metal(II) complexes using agarose gel electrophoresis method. The reaction mixture containing 20 µL of PUC18DNA in 50 mM, Tris-HCl, pH 7.4, 52 mM, NaCl, 10 mM of H_2O_2 were added in a different volume and then adding the millipore water for final volume. The mixed solutions were incubated at 37 °C for 1 h. After adding 0.5 g powdered agarose to 50 mL of buffer solution, it is heated, then cooled and added to ethidium bromide. The gel was examined under ultraviolet light and photographed[22].

Antioxidant assay

The antioxidant assay of all synthesised compounds were investigated by using 2,2'-diphenyl-2-picrylhydrazyl radical (DPPH) scavenging method. The tested compounds were dissolved in DMSO and DPPH (50 µL, 0.6 mM) in methanol solution. The reaction mixture was prepared at various concentrations (10, 20, 30, 40, 50 µL). The solutions were incubated at room temperature for 20 min in dark place and read the absorbance at 517 nm. DPPH used as a blank solution as well in varying concentrations[23]. The percentage inhibitory of DPPH scavenging was calculated by the following equation.

$$\text{Percentage of inhibition} = [(A_0\text{-}A_1)/A_0] \times 100$$

Where, A_0 is the absorbance of the control and A_1 is the absorbance of the sample. The IC_{50} (concentration of sample required to scavenge 50% free radical or to prevent lipid peroxidation by 50%) was calculated from the regression equation.

MTT assay of cytotoxicity

In vitro cytotoxicity MTT [3-(4,5-dimethylthiazol-2-yl)-2,5-diphenyltetrazolium bromide] assay of Cu(II) complexes were determined by using human MCF-7 cell line at 24 h of drug administration in different concentration. The stock solution of tested complexes were prepared from 1% DMSO diluted with medium. The monolayer cell line was cultured in 96 well microtiter flat plate in DMEM medium supplemented with 10% inactivated Fetal Bovine Serum (FBS), Penicillin (100 units/mL) and Streptomycin (100 µg/mL) in a humidified at 37 ºC, 5% CO_2 atmosphere incubated for 24 h. The incubation was continued for 24 h when adding the tested complexes in various dilutions and cell counts was adjusted to 1×10^5 cell/mL and suspended on the plate. To find out the viability cells, spread solution of 0.2% Trypsin, 0.02% EDTA and 0.05% glucose in PBS were added when adding with tested complexes. The absorbance was recorded by Shimadzu UV-visible spectrometer at 570 nm region of wavelength. Average values and percentage ratio were calculated through three times of independent experiments[24]. By non-linear regression equation gives the maximum inhibition concentration IC_{50} values on dose-dependent manner.

Results and Discussion

The synthesised ligands N,N'-1,2-phenylenebis (methylidene))bis(4-hydroxybenzohydrazide) **1** and N, N'-1,3-phenylenebis (methylidene))bis(4-hydroxybenzo hydrazide) **2** with their complexes are coloured and stable in air at room temperature. The elemental analytical data (Table 1) reveals that the metal complexes co-ordinates with ligand in 1:1 molar ratio. The molar conductance values of 10^{-3} M concentration in DMF solution are obtained in range 7.5-18.4 $\Omega^{-1}cm^2mol^{-1}$. These values indicate that the non-electrolytic nature of the metal complexes[25].

The infrared spectral data furnished the characteristic vibration modes and functionality of different groups of ligands and their complexes were synthesised. The infrared spectrum gave the valuable intensity regions are listed in Table 2 (Supplementary Data, Fig. S1 and S2). The characteristic sharp absorption bands of free ligand **1** appear at 1546 cm^{-1} and ligand **2** appear at 1582 cm^{-1} due to stretching vibrations of azomethine (CH=N) group[26]. For complexes the absorbance bands are shifted to longer wavelength at 54-60 and 12-24 cm^{-1}, likely to be co-ordination of metal ions with sharing of lone pair electrons of azomethine nitrogen atom. The ligands (C=O) stretching vibrations of medium bands displays at 1671 and 1662 cm^{-1}. For complexes, these bands are highly shifted to their wavelength 65-35 and 77-10 cm^{-1} which denotes the participation of co-ordination of metal ions with oxygen donor of carbonyl group.

In lower frequencies, the complexes exhibit two small intensity bands in range of (M-O) and (M-N) stretching vibrations, while M-O stretching absorbance bands exhibited at 553-485 cm^{-1} and M-N stretching band appeared at 452-422 cm^{-1}. The ligands **1** and **2** exhibited the broad band of intensity in the

region at 3318 and 3371 cm^{-1} for stretching vibration of OH and another band appeared at 3174 and 3078 cm^{-1} for NH stretching vibration[27]. These bands are slightly changed for all formed complexes; indicate the non-involvement of co-ordination with metal ions and shows free manner of OH and NH groups.

The proton nuclear magnetic resonance spectrum of ligands **1** and **2** gave the characteristic singlet signal of CH=N group found to be at δ 8.54-8.49 ppm as shown in Fig. 1. In downfield shifts of the two sharp singlet signals appeared at δ 10.45-10.16 ppm and δ 11.79-11.47 ppm due to presence of hydroxyl and NH protons. The multiplet signals of aromatic phenyl protons appeared at δ 7.8-7.5 ppm and δ 6.82-6.90 ppm of chemical shifts[28]. This signal of peaks shows the purity of ligands.

The mass spectra gave the promising results and used for elucidate the molecular structures of ligands and its metal complexes as shown in Fig. 2 and in Supplementary Data, Fig. S3 and S4. The ligand **1** exhibited the molecular ion peak M^+ at m/z = 403.14 amu due to $[M+1]^+$ and its complexes showed the peak at 531.38 $[M]^+$, 531.85 $[M]^+$, 537.44 $[M+1]^+$, 539.99 $[M+2]^+$. Also ligand **2** exhibited the molecular ion peak M^+ at m/z = 403.14 amu and its complexes showed the base peak at 531.38 $[M]^+$, 533.37 $[M+1]^+$, 537.29 $[M+1]^+$, 541.44 $[M+4]^+$. The various fragmentations indicate the stability of the complexes and moreover, the obtained results are good agreement with the proposed structure of molecular formulae.

The electronic spectra of ligands and its complexes values are listed in Table 3. The ligand **1** shows that

Table 1 — Elemental analytical data of ligand 1, 2 and their complexes

Molecular formula	Molecular weight	Colour	Melting point (°C)	Elemental analysis calculated (found) %			Conductivity (Ω^{-1} cm^2 mol^{-1})
				C	H	N	
$C_{22}H_{18}N_4O_4$ $[L_1]$ **1**	402	Sandal	185	65.66 (64.90)	4.51 (4.31)	13.92 (13.34)	-
$C_{22}H_{18}N_4O_4$ $[L_2]$ **2**	402	White	192	65.66 (64.65)	4.51 (4.46)	13.92 (13.74)	-
$CoC_{22}H_{18}N_4O_4Cl_2$ $[CoL_1Cl_2]$ **1a**	531.9	Pale green	249	49.63 (48.31)	3.41 (3.20)	10.53 (9.93)	14.2
$NiC_{22}H_{18}N_4O_4Cl_2$ $[NiL_1Cl_2]$ **1b**	531.7	Greenish yellow	278	49.65 (49.23)	3.41 (3.52)	10.53 (10.01)	7.5
$CuC_{22}H_{18}N_4O_4Cl_2$ $[CuL_1Cl_2]$ **1c**	536	Green	301	49.20 (48.54)	3.38 (3.91)	10.44 (9.86)	17.5
$ZnC_{22}H_{18}N_4O_4Cl_2$ $[ZnL_1Cl_2]$ **1d**	538	White	265	49.03 (49.25)	3.37 (3.18)	10.40 (9.65)	11.0
$CoC_{22}H_{18}N_4O_4Cl_2$ $[CoL_2Cl_2]$ **2a**	531.9	Blue	256	49.63 (47.64)	3.41 (3.12)	10.53 (9.49)	13.7
$NiC_{22}H_{18}N_4O_4Cl_2$ $[NiL_2Cl_2]$ **2b**	531.7	Greenish yellow	287	49.65 (49.01)	3.41 (3.61)	10.53 (10.71)	9.6
$CuC_{22}H_{18}N_4O_4Cl_2$ $[CoL_2Cl_2]$ **2c**	536	Green	312	49.20 (48.81)	3.38 (2.91)	10.44 (10.54)	18.4
$ZnC_{22}H_{18}N_4O_4Cl_2$ $[ZnL_2Cl_2]$ **2d**	538	Ash white	275	49.03 (47.59)	3.37 (3.43)	10.40 (9.91)	10.3

Table 2 — IR spectral values of ligands 1, 2 and their complexes

Compound	(OH)	(NH)	(C=O)	(CH=N)	(M-O)	(M-N)
1	3318	3174	1671	1546	-	-
2	3371	3078	1662	1582	-	-
1a	3264	2922	1689	1602	495	431
1b	3244	2961	1724	1605	550	452
1c	3217	2983	1680	1600	496	422
1d	3309	2924	1736	1606	554	452
2a	3243	3174	1657	1606	492	430
2b	3252	3173	1652	1603	485	447
2c	3261	3169	1739	1604	546	423
2d	3280	3176	1672	1594	553	429

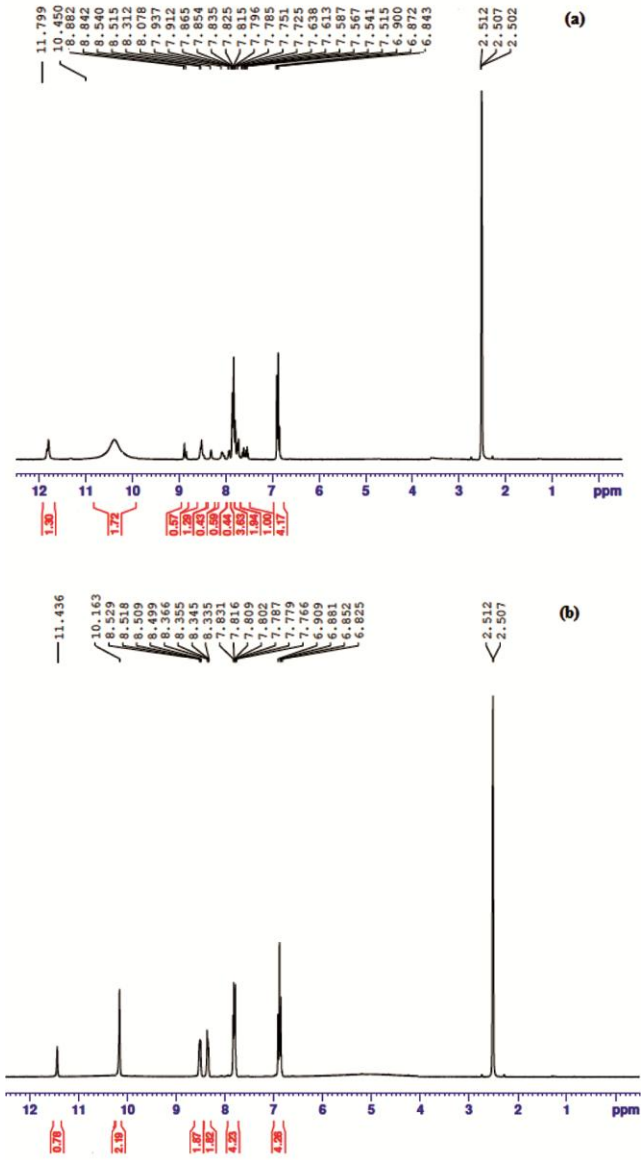

Fig. 1 — ^{1}H NMR spectra of ligand (a) **1** and (b) **2**

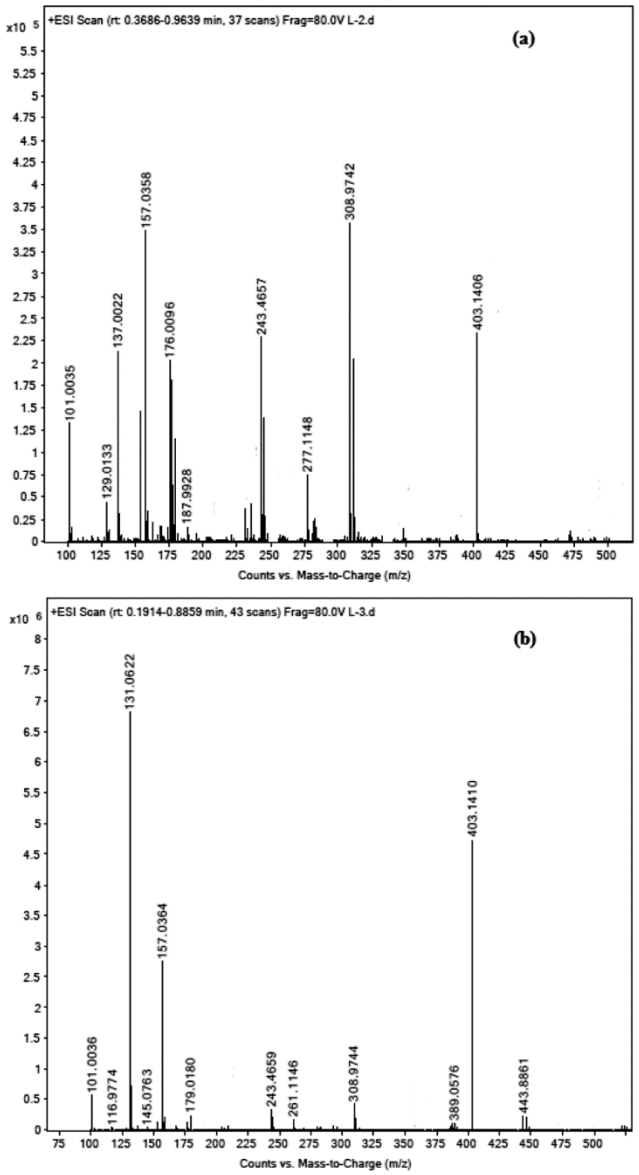

Fig. 2 — Mass spectra of ligand (a) **1** and (b) **2**

the two absorption bands at 298, 317 nm and ligand **2** shows bands at 281, 306 nm corresponding to π→ π* and n→π* transitions, respectively. The charge transfer band of all complexes appears at 432-362 nm indicates ligands co-ordinated to metal ions. The absorption spectrum of complexes **1a** and **2a** display the characteristics intensity bands at 608, 675 nm and 608, 674 nm, which are assigned to $^{3}A_{2g}$ (F) → $^{3}T_{2g}$ (F) (ϑ_1), $^{3}A_{2g}$ (F) → $^{3}T_{1g}$ (F) (ϑ_2) and $^{3}A_{2g}$ (F) → $^{3}T_{1g}$ (P) (ϑ_3) transitions, respectively.

The magnetic momentum of both complexes lie at 3.62 BM and 3.53 BM, which confirmed the octahedral environment around the Co(II) ion[29,30]. The complex **1b** gave the characteristic bands at 452, 562 nm, and **2b** complex gave the bands at 452, 608 nm which attributed to transition of $^{3}A_{1g}$ (F) → $^{3}T_{1g}$ (P) and $^{3}A_{1g}$ (F) → $^{3}T_{2g}$ (F), respectively, and the magnetic moment values fall on the range at 3.24 BM and 3.21 BM suggested that the octahedral structure of the both Ni(II) ion[31]. The intensity bands shows at 432 nm for the complex **1c** while the complex **2c** gave the bands at 438, 538 nm assigned to $^{2}E_{g}$ → $^{2}T_{2g}$ and $^{2}B_{1g}$→ $^{2}A_{1g}$ transitions, respectively, and the magnetic moment 1.91 BM and 1.89 BM values reported the distorted octahedral geometry due to ligand field and Jahn-Teller effects[32,33]. The diamagnetic nature and the empirical formulae of formed complexes **1d** and

Table 3 — Electronic spectra and magnetic data of ligand 1, 2 and their complexes

Compounds	Electronic spectra (nm)				Transitions	Geometry	Magnetic moments
	π→π*	n→π*	L→M	d-d			
1	298	317	-	-	-	-	-
2	281	306	-	-	-	-	-
1a	296	318	402	608 675	^{3}A2g (F) → ^{3}T2g (F) ^{3}A2g (F) → ^{3}T1g (F) ^{3}A2g (F) → ^{3}T1g (P)	Octahedral	3.62
1b	308	347	371	452 562	^{3}A1g (F) → ^{3}T1g (P) ^{3}A1g (F) → ^{3}T2g (F)	Octahedral	3.24
1c	302	321	341	432	^{2}B1g→ ^{2}A1g	Distorted octahedral	1.91
1d	294	342	432	-	-	Octahedral	-
2a	281	370	379	608 674	^{3}A2g (F) → ^{3}T2g (F) ^{3}A2g (F) → ^{3}T1g (F) ^{3}A2g (F) → ^{3}T1g (P)	Octahedral	3.53
2b	290	371	389	452 708	^{3}A1g (F) → ^{3}T1g (P) ^{3}A1g (F) → ^{3}T2g (F)	Octahedral	3.21
2c	284	300	362	438 548	^{2}Eg → ^{2}T2g ^{2}B1g→ ^{2}A1g	Distorted octahedral	1.89
2d	287	302	370	-	-	Octahedral	-

2d proposed the octahedral arrangement around the Zn(II) ion.

The X-band ESR spectra of the complexes **1c** and **2c** were recorded in polycrystalline state at room temperature under the magnetic field (G) shown in Fig. 3. The ESR spectra of complex **2c** gave the isotropic signal with no hyperfine splitting and the parameters of g_{II}, $g_{\perp}$ and g_e (2.0023) values are listed in Supplementary Data, Table S1. In results, $g_{II} > g_{\perp}$ suggested that the axially elongated octahedral, and an unpaired electron of d^9 configuration predominantly present in d_{x2-y2} orbital. Meanwhile the complex **1c** shows the super hyperfine structure split into three lines due to the ligand N strongly binds to metal atom and form Cu-N bond. This shows that the unpaired electron delocalized through the whole geometry[34].

According to Hathway[35] expression (G) = $(g_{II}-2)/(g_{\perp}-2)$ gives the coupling interaction between the two Cu(II) ion. When G < 4.0, indicates to there is no coupling interaction between the presenting Cu(II) ion. The ESR result of (**1c**, **2c**) shows that $g_{II} > 2.3$ indicating the complexes are covalent in nature[36].

The thermal stabilities of complexes were studied using TG and DSC analysis at heating rate of 20 ºC/min in air. The representative TG-DSC curves of complexes are shown in Fig. 4. The thermal decomposition of **1a** occurs in two steps. The first thermal degradation occurred between 64-177 °C followed by an endothermic DSC peak observed in 79 °C. This observed mass loss was attributed to the loss of chloride ions. The second stage of thermal degradation in 367 °C corresponds to decomposition of ligand from metal chelates. The thermal degradation of complex **2c** occurred between in 112-232 ºC and followed by DSC peak observed in 104 ºC. This observed mass loss was attributed to the loss of chloride ions. The further second stage degradation occurs in 301 °C corresponds to decomposition of ligand from metal complex. Inspite of that, observed horizontal lines in the TGA curves of beyond 549 °C and 525 °C of the complex **1a**, **2c** indicates no further weight loss, implying that metal

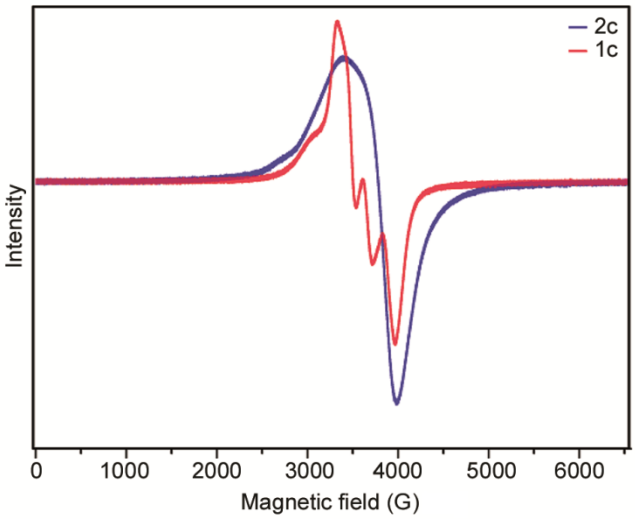

Fig. 3 — Electron spin resonance spectra of complex (a) **1c** and (b) **2c**

oxides may be final residue. Similar types of results are obtained for other complexes; the thermal analysis results are consistent with the elemental analysis findings.

Molecular docking

Molecular docking is preeminent technique in structure based drug design to understand mechanism of ligand recognition and specific and thereby giving an insight into presumable protein-ligand interactions and binding affinity. Affinity of molecules to antibacterial receptors is very important in drug design. Therefore we carried out molecular docking of ligands with target protein (PDB ID: 2DHN). The molecular interactions of ligands for inhibition against *Staphylococcus aureus* protein represented in Fig. 5. According to this interaction, the ligand (**1**, **2**) shows interactions with the active site residues (THR51,

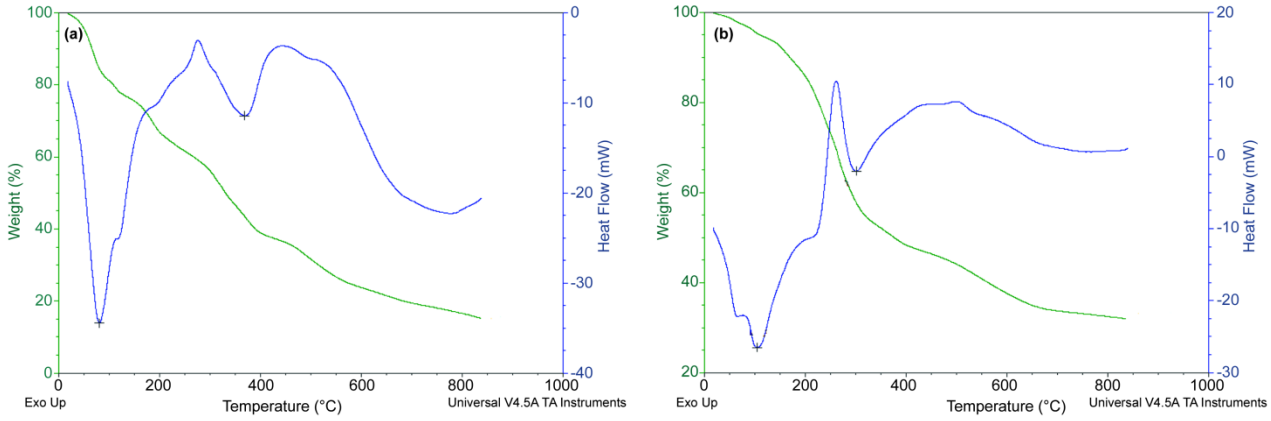

Fig. 4 — TGA/DSC curves of complex (a) **1a** and (b) **2c**

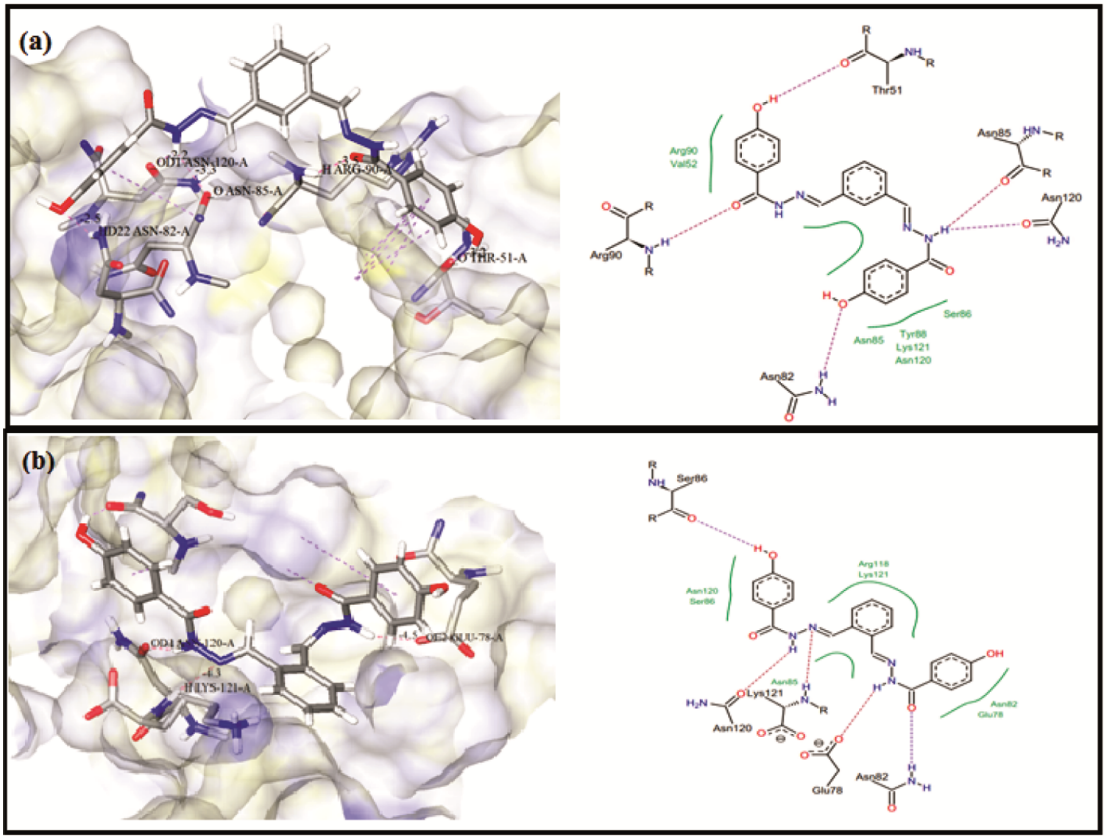

Fig. 5 — Pictorial representation of possible binding sites of ligands (a) **1** and (b) **2**

ARG90, ASN82, ASN85 & GLU78, ASN120, ASV121) and the obtained inhibition energy was -22.32, -18.81 kcal/mol. This more negative value of estimated free energy of binding represents more efficient binding of ligands with target protein.

In vitro antibacterial study

The antimicrobial activities of all formed complexes were tested against pathogens of *S. aureus*, *B. substilis*, *K. pneumoniea* and *E. coli* bacterial strains[37]. All tested metal complexes having higher potential activity than the free Schiff base ligands (Table 4). As compared to all screened bacterial strains, the strain of *E. coli* showed better activity. The complexes **1c**, **2a** and **2c** gave efficient activity with tested pathogens than other complexes. The poor activity was showed by the complexes **1a** and **2b**. This was an explained on basis of chelation theory. It concludes that the antimicrobial activity was enhanced by complexation. In metal chelates, the polarity of central metal is decreased because partial sharing of its positive charge with associated donor groups of ligand and chelation enhances an electron delocalization over the whole chelating ring. It could be facilitate ability of the complexes to cross a lipid membrane of pathogens and form the hydrogen bonds with the imine groups of the active sites. This formation damages the cell membrane and causes to cell death[38].

Table 4 — Antibacterial activities of synthesised ligands and their complexes

Compounds	Zone of inhibition in 100µg/mL (nm)			
	Gram positive bacteria		Gram negative bacteria	
	S. aureus	*B. subtilis*	*K. pneumoniea*	*E. coli*
1	-	-	-	-
2	-	-	-	-
1a	6	8	6	3
1b	8	9	8	7
1c	9	10	11	8
1d	9	10	9	8
2a	10	12	10	9
2b	5	8	5	7
2c	12	13	12	10
2d	8	12	10	7
Tetracycline	15	14	17	10

In vitro antioxidant activity

The antioxidant of all synthesised compounds were tested by using 1,1'-diphenyl-1-picrylhydrazyl (DPPH) radical assay. The DPPH assay is widely used to determine the antioxidant capacity of bio-metal compounds. DPPH radical is stable in normal conditions, but it combined with complexes donate an electron leads to destruction of the radical. All complexes show good inhibition activity than ligands when compared to standard. IC_{50} values of (**1**, **2**, **1a-2d)** compounds and ascorbic acid are 40.99, 40.01, 34.00, 22.41, 27.88, 39.90, 35.69, 24.52, 23.21, 38.21 and 57.68 µg/mL. Commonly, the lower value of IC_{50} indicates the higher antiradical capacity and the complexes **1c** and **2c** has high potential antioxidant activity leads to destruction the free radicals[39].

UV-visible absorbance binding study

The complexes (**1c**, **2c)** were monitored by the binding mode of interaction with ct-DNA using UV-visible absorbance titrations study. The binding ability of complexes in the absence and presence of ct-DNA was shown in Fig. 6. The absorbance gave the intense band at 259 nm for complex **1c** and band at 260 nm for **2c** assigned to be $\pi \rightarrow \pi^*$ transition of aromatic chromophore[40]. In general, in ligands, the aromatic moieties are bind with DNA, through a intercalation

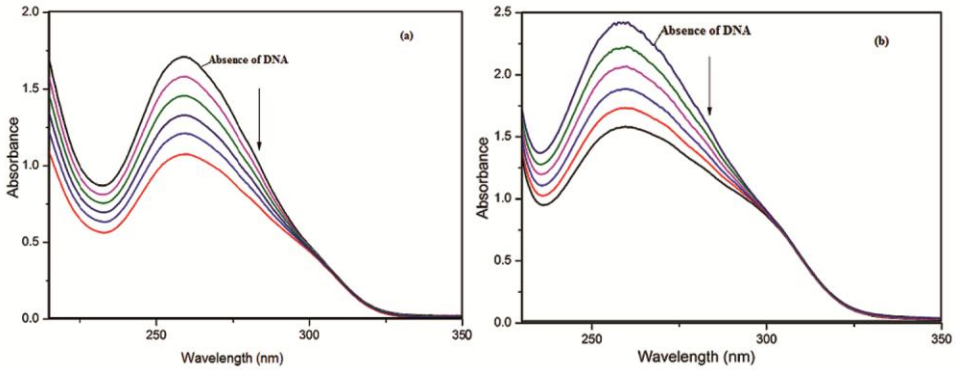

Fig. 6 — UV-visible titrations of (a) **1c** and (b) **2c** in the absence and presence of 100, 120, 140, 160 and 180 µM of ct-DNA

binding which results to give hypochromism with red shift and azomethine group damage the double helix of DNA, which results in hyperchromism. It exhibits the strong $\pi \rightarrow \pi^*$ stacking interaction between the aromatic chromophore ligand of metal complex and the base pairs of DNA. Addition of DNA with both complexes in increasing concentration (120, 140, 160, 180, 200 µM) the bands are shifted to red approximately to 3, 5, 7, 9, 11 nm, respectively. These changes of complexes suggest that the binding interaction of complexes with DNA might to be intercalative mode [41] of hypocromism with red shifts.

Electrophoresis of DNA cleavage activity

The efficiency of all synthesised compounds to cleavage DNA was performed by gel electrophoresis using compact supercoiled plasmid PUC18DNA in ammonium acetate buffer at pH 7.5. Compact plasmid DNA was subjected through the gel electrophoresis, the fastest moving will be observed for supercoiled Form **I** (SC). If one strand of supercoil is cleaved, it will generates slow moving nicked Form **II** (NC) and both strands are cleaved, it will be converted to linear Form **III** (L) moves in between Form **I** and Form **II**[42]. Cleavages of PUC18DNA with increasing concentration of metal complexes in the presence of hydrogen peroxides are shown in the Fig. 7.

During electrophoresis the plasmid DNA is not affected when the successive addition of complex **2a**.

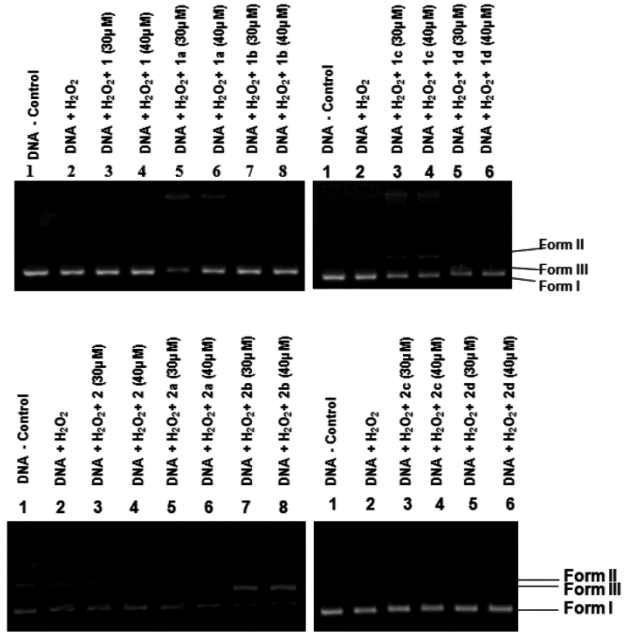

Fig. 7 — Oxidative DNA cleavages of ligands and its complexes in presence of hydrogen peroxide

Meanwhile, the tested compounds break DNA molecule in the presence of peroxide, due to formation of hydroxyl ($^{\bullet}OH$) radicals. These free radicals induces the pair of redox reactions between the partially reduces peroxide and the metal compounds and also participate in the oxidation of deoxyribose moiety, followed by hydrolytic cleavage of the sugar phosphate backbone[43,44]. The ligands (**1**, **2**) and the complexes (**1a, 1b, 1d, 2a, 2b**, **2d)** with supercoil PUC18DNA, gel electrophoresis migrates faster to produce Form **I** (SC) and then converted to Form **II** (NC). Eventhough, the complexes (**1c**, **2b)** cleave both strands of DNA successfully to form **III** (L) with slow migration between SC and NC. The efficient cleavage reduces the formation of free radicals and can be used as cancer treatment agents[45].

Anticancer activity

The cytotoxicity of complexes **1c** and **2c** of MCF-7 cell line revealed that the IC_{50} values of 36.88 µM and 57.56 µM shown in the Table 5 (Fig. 8). The lower inhibitory value of IC_{50} exhibits higher toxicity of complexes. The obtained inhibitory values are compared with the other studies, found to mostly greater cytotoxic effects towards the human MCF-7 cell line[46,47]. This anticancer activity of complexes may be attributed to planarity and the enhancement of coordination of Cu(II) ion around the aromatic ring system and position of azomethine group. During the coordination of the complexes, positive charge of metal(II) ion increases due to donor group of ligands[48]. This leads to enhance the higher anticancer activity against MCF-7 cells.

Table 5 — Anticancer activity of Schiff base ligand and its % of cell inhibition at various concentrations

Compound	Concentration (µg/mL)	% of cell inhibition	IC_{50} (µg/mL)
Control	0	0.791	-
	100	14.34	
1c	200	34.72	36.88
	400	53.98	
	600	71.47	
	800	76.58	
	1000	84.87	
	100	9.78	
2c	200	24.45	57.56
	400	43.64	
	600	59.76	
	800	65.76	
	1000	74.84	

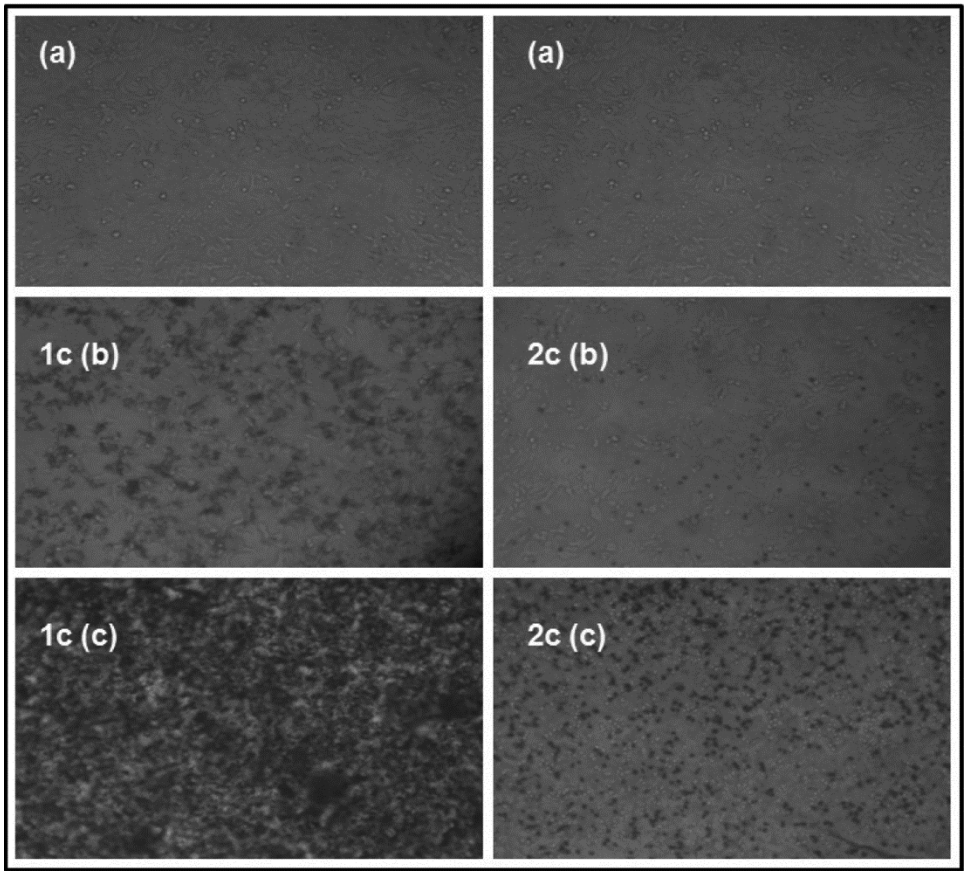

Fig. 8 — Phase-contrast image changes (a) control (MCT-7 cells), (b) complex (**1c**, **2c)** 100 µM and (c) complex (**1c**, **2c)** 1000 µM

Conclusions

In our present work, the new eight complexes synthesised and derived isomeric form of two bis-Schiff base ligands, namely N,N'-1,2-phenylenebis (methylidene))bis(4-hydroxybenzohydrazide) **1** and N,N'-1,3-phenylenebis(methylidene))bis(4-hydroxyb enzohydrazide) **2** are characterised by analytical and spectroscopic techniques. The analytical calculation and mass analyses confirmed the molecular formulae of complexes and assigned to coordination of metal with ligand in 1:1 molar ratio. The more binding interaction showed by ligand **1** due to position of 1, 3 isomer. The metal complexes showed sustainable antimicrobial effects than the parent Schiff base ligand. The UV-visible absorbance titrations of **1c** and **2c** complexes results show that the non-covalent interaction is possible to intercalative mode of binding with ct-DNA. However, the complexes **1c** and **2c** posses effective cleavage and cleave double-strands of PUC18DNA in the presence of hydroxyl radicals with increasing concentration. Antioxidant assay of DPPH radical activity revealed that all complexes gave the considerable potential effects. Cytotoxicity of complexes exhibited the valuable therapeutic properties against the MCF-7 cancerous cell line.

Supplementary Data

Supplementary data associated with this article are available in the electronic form at http://nopr.niscair.res.in/jinfo/ijca/IJCA_60A(07)915-926_Supp lData.pdf.

References

1 Mohammadizadeh F, Khanamani S, Rezaei A, Mohamadi M, Hajizadeh M.R, Mirzaei M.R, Khoshdel A, Fahmidehkar M A & Mahmoodi M, *Biometal*, 31 (2018) 233.
2 Jayaseelan P, Prasad S, Vedanayaki S & Rajavel R, *Arabian J Chem*, 9 (2016) S668.
3 Zheng K, Jiang L, Li Y, Wu Z & Yan C, *RSC Adv*, 5 (2015) 51730.
4 Du Y, Chen W, Fu X, Deng H & Deng J, *RSC Adv*, 6 (2016) 109718.
5 Bruijnincx P C A & Sadler P J, *Curr Opin Chem Biol*, 12 (2008) 197.
6 Gholivand M B, Kashanian S & Peyman H, *Spectrochim Acta Part A*, 87 (2012) 232.
7 Mishra M, Tiwari K, Shukla S, Mishra R & Singh V P, *Spectrochim Acta Part A*, 132 (2014) 452.

8 Li Y, Yang Z, Zhou M, Li Y, He J, Wang X & Lin Z, *RSC Adv*, 7 (2017) 41527.
9 Kumar C V, Barton J K & Turro N J, *J Am Chem Soc*, 107 (1985) 5518.
10 Banerjee S, Patra R, Ghorai P, Brandão P, Chowdhury S G, Karmakar P & Saha A, *New J Chem*, 42 (2018) 16571.
11 Harinath Y, Kumar D H, Kumar B N, Apparao C & Seshaiah K, *Spectrochim Acta Part A*, 101 (2013) 264.
12 Burgos-Lopez Y, Del Plá J, Balsa L M, León I E, Echeverría G A, Piro O E, García-Tojal J, Pis-Diez R, González-Baró A C & Parajón-Costa B S, *Inorganic Chim Acta*, 31 (2019) 487.
13 Tyagi M, Tyagi P & Chandra S, *Appl Organometal Chem*, 31 (2017) e3880.
14 Malik M A, Dar O A, Gull P, Wani M Y & Hashmi A A, *Medchemcomm*, 9 (2018) 409.
15 Manikandan R, Viswanathamurthi P & Muthukumar M, *Spectrochim Acta Part* A, 83 (2011) 297.
16 Arjunan V, Rani T, Mythili C V & Mohan S, *Spectrochim Acta Part A*, 79 (2011) 486.
17 El-boraey H A, El-domiaty A M & El-kom S, *J Adv Chem*, 16 (2019) 6313.
18 Naik K H K, Raj S & Naik N, *Spectrochim Acta Part A*, 131 (2014) 599.
19 Kostova I & Momekov G, *Eur J Med Chem*, 43 (2008) 178.
20 Pelczar M J, Chan E C S, Krieg N R, *Microbiology*, Fifth ed, (Tata McGrawHill Publishing Co., Ltd, New Delhi), 1998.
21 Felsenfeld G & Hirschman S Z, *J Mol Biol*, 13 (1965) 407.
22 Neelakantan M A, Rusalraj F, Dharmaraja J & Johnsonraja S, *Spectrochim Acta Part A* , 71 (2008) 1599.
23 Blois M S, *Nature*, 181 (1958) 1199.
24 Mosmann T, *J lmmunol Methods*, 65 (1983) 55.
25 Geary W J, *Coord Chem Rev*, 7 (1971) 81.
26 Chandra S & Kumar S, *Spectrochim Acta Part* A, 135 (2015) 356.
27 Hernández-gil J, Ferrer S, Cabedo N, López-gresa M P, Castiñeiras A & Lloret F, *J Inorg Biochem*, 125 (2013) 50.
28 Anitha C, Sumathi S, Tharmaraj P & Sheela C D, *Inter J Inorg Chem*, 2011 (2011) 1.
29 Ballhausen C J, *Introduction to Ligand Field Theory*, (McGraw–Hill, New York), 1962.
30 Dhahagani K, Kumar S M, Chakkaravarthi G, Anitha K, Rajesh J, Ramu A & Rajagopal G, *Spectrochim Acta Part A*, 117 (2014) 87.
31 Sikarwar P, Tomar S & Singh A P, *Am J Chem*, 6 (2016) 119.
32 Lever A B P, *Inorganic Electronic Spectroscopy*, 2nd ed., (Elsevier, Amsterdam, The Netherlands), 1984.
33 Kolhe N H & Jadhav S S, *Res Chem Intermed*, 45 (2019) 973.
34 Kozlevcar B & Segedin P, *Croat Chem Acta*, 81 (2008) 369.
35 Hathaway B J & Billing D E, *Coord Chem Rev*, 5 (1970) 143.
36 Kivelson D & Neiman R, *J Chem Phy*, 35 (1961) 149.
37 Turkoglu A, Emin M & Mercan N, *Food Chem*, 101 (2007) 267.
38 Tweedy B G, *Phytopathology*, 55 (1964) 901.
39 Chohan Z H, Arif M, Akhtar M A & Supuran C T, *Bioinorg Chem Appl*, 2006 (2006) 1.
40 Krishnamoorthy P, Sathyadevi P, Butorac R R, Cowley A H, Bhuvanesh N S P & Dharmaraj N, *Dalton Trans*, 41 (2012) 6842.
41 Nitha L P, Aswathy R, Elsa N, Sindhu B & Mohanan K, *Spectrochim Acta Part A*, 118 (2014) 154.
42 Barton J K, Danishefsky A T & Goldberg J M, *J Am Chem Soc*, 116 (1984) 2172.
43 Borowska J, Sierant M, Sochacka E & Sanna D, *J Biol Inorg Chem*, 20 (2015) 989.
44 Okagu O D, Ugwu K C, Ibeji C U, Ekennia A C, Okpareke C, Ezeorah C J, Anarado C J O, Babahan I, Yıldız U, Cömert F & Ujam O T, *J Mol Struct*, 1183 (2019) 107.
45 Lee W Y, Yan Y K , Lee P P F, Tanb S J & Limb K H, *Metallomics*, 4 (2012) 188.
46 Yaghobi Z, Ranjbar Z R & Gharbi S, *Polyhedron*, 164 (2019) 176.
47 Petrovic V P, Živanovic M N, Simijonovic D, Dorovi J, Petrovic Z D & Markovic S D, *RSC Adv*, 105 (2015) 86274.
48 Uysal S & Erdem Koç Z, *J Mol Struct*, 1109 (2016) 119.